Malaysian Journal of Analytical Sciences (MJAS)
Published by Malaysian Analytical Sciences Society

CURRENT PROGRESS IN DYE-SENSITISED SOLAR CELLS (DSSCs) FEATURING DONOR-π-ACCEPTOR SYSTEM OF MIXED MOIETIES: A REVIEW

(Kemajuan Terkini Sel Suria Peka Cahaya (DSSCs) Menampilkan Sistem Moiti Campuran Penderma-π-Penerima: Satu Ulasan)

Wan M. Khairul[*]*, and Muhammad Aidil Zailani*

Faculty of Science and Marine Environment,
Universiti Malaysia Terengganu, 21030 Kuala Nerus, Terengganu, Malaysia

[*]*Corresponding author: wmkhairul@umt.edu.my*

Received: 27 July 2023; Accepted: 13 September 2023; Published: 30 October 2023

Abstract

In recent years, the quest to propose an ideal molecular system acting as dye-sensitised solar cells (DSSCs) bearing single molecular system have attracted great interest. This is due to their promising potential to convert solar energy into electrical energy at low cost. The alteration of molecular framework is essential to propose a rigid rod donor-π-acceptor system in enhancing its electronic properties to be applied as active layer in this type of solar cells. In recent years, mixed moieties molecules are actively being proposed as this combination proven to provide better performance of efficiency. However, the molecules bearing different moieties with different atomic features are rather scarce. The extended conjugation and the push-pull phenomenon within the molecular backbones may provide efficient electronic properties with alteration from different substituents. The development of DSSCs featuring conjugated mixed moieties are relatively new and scarce. Thus, this review article provides an insight general idea on the fundamental aspects of DSSCs as its progresses in term of its essentials features and compositions which focusing on the utilisation of these moieties. It is hope that this contribution may equip one's understanding in venturing similar work on this type of molecular system.

Keywords: DSSCs, conjugation, donor-π-acceptor, acetylene, azomethine

Abstrak

Sejak kebelakangan ini, pencarian untuk mencadangkan sistem molekul unggul yang bertindak sebagai sel suria peka cahaya (DSSC) menampilkan system molekul tunggal telah menarik perhatian yang tinggi. Ini adalah disebabkan kerana ia menjanjikan potensi untuk menukar tenaga suria kepada tenaga elektrik pada kos yang rendah. Pengubahsuaian kerangka molekul adalah penting bagi mencadangkan sistem penderma-π-penerima rod tegar dalam meningkatkan sifat elektroniknya untuk diaplikasikan sebagai lapisan aktif dalam sel suria ini. Sejak beberapa tahun lalu, molekul-molekul tercampur moiti secara aktifnya banyak dicadangkan kerana penggabungan ini telah membuktikan prestasi keberkesanan yang baik. Walau bagaimanapun, molekul-molekul yang menampilkan moiti berbeza dengan tampilan atom berlainan adalah amat jarang. Pemanjangan konjugasi dan fenomena tolak-tarik di dalam kerangka molekul mampu menyediakan sifat elektronik berkesan melalui pengubahsuian daripada pelbagai kumpulan pengganti. Pembangunan DSSC yang menonjolkan campuran moiti terkonjugat ialah agak baharu dan jarang dilaporkan. Oleh yang demikian, artikel ulasan ini menyediakan hala tuju idea secara umum terhadap aspek-aspek asas DSSC dan

kemajuannya befokuskan ciri-ciri penting dan komposisinya yang memfokuskan penggunaan moiti-moiti ini. Diharapkan agar sumbangan ini dapat menlengkapkan pemahaman seseorang dalam penglibatan kerja yang sama terhadapa sistem molekul jenis ini.

Kata kunci: DSSC, konjugasi, penderma-π-penerima, asetilina, azometina

Introduction

The sun is the single most vital energy provider for life on Earth. It provides energy to plants and planktons for photosynthesis process. In turn, the planktons and plants are then consumed by animals, providing energy for them. Almost all of the electricity that we use nowadays is also provided by the sun, albeit not in a straightforward way. Examples are wind energy caused by movement of air due to heat from the sun, hydropower energy that derived energy from water that fell as rain after being evaporated by the sun, and also fossil fuels, which are formed from the biomass of animals and plants [1]. Through the use of photovoltaic cells or solar cells, energy in sunlight can also be directly harvested to obtain electricity.

Sunlight is a form of electromagnetic radiation, consisting of 56% infrared, 36% visible and 7% ultraviolet radiation, with the remainder consisting of other electromagnetic radiations [1]. Earth received around 1.8 x 10^{14} kW of energy from sunlight. When sunlight hits the earth's atmosphere, around 40% of the sunlight is reflected back into space or absorbed by the atmosphere, so around 60 % or 1.08 x 10^{14} kW reaches the earth's surface [2]. The absorption of sunlight is due to molecules in the atmosphere such as water, carbon dioxide, ozone and oxygen. Water and carbon dioxide absorb the infrared radiation while ozone and oxygen absorb the ultraviolet radiation, thus changing the composition of the sunlight reaching the earth's surface to comprise of around 50% visible radiation and 47% infrared. The sunlight reaching earth's surface exists in two forms, direct radiation and diffuse radiation, with the latter resulted from the many scattering and absorption processes occurring when the sunlight travels through the atmosphere [1].

The total amount of energy from the sun reaching the earth's surface is around 3.4 x 10^{6} EJ [1], which is several thousand times the global energy consumption in 2019, which is 173,340 TWh [3], or around 624 EJ. Thus, there is tremendous potential in directly harnessing solar energy through photovoltaic cells for our future energy needs.

Development of dye-sensitised solar cells (DSSCs)

History of solar cells

Solar cells generate power via photovoltaic effect in which sunlight is converted into electrical current. Photovoltaic effect was first observed by Alexandre Edmond Becquerel in 1839. His cell was a wet cell, with either silver chloride or silver bromide coated electrodes immersed in acidic solution and contained within a black container. He observed that the voltage of the cell increased when its silver electrodes were exposed to sunlight [4]. In 1883, Charles Fritts as can be observed in Figure 1 created the first solar cell using selenium coated with a thin layer of gold, but its efficiency was only around 1% [5].

In 1946, Russel Ohl patented the first p-n junction silicon solar cell. He noticed that a silicon sample with a crack had current flowing in it when exposed to light. The crack formed at the boundary between the positively and negatively-doped part of the silicon, and when connected to a circuit, the photon in light imparts energy to the electron building up on the negatively-doped part to flow to the positively-doped part, thus generating electrical current. But the solar cell's efficiency was only 1% [6]. The first practical solar cell was developed by Daryl Chapin, Calvin Fuller and Gerald Pearson from Bell Labs in 1954. They first discovered that silicon with lithium and gallium impurities became very sensitive to light. They experimented with different impurities to further improve their silicon solar cells, and resulted in the use of boron and arsenic as the doping materials for their silicon solar cells, with efficiency of 6% [6].

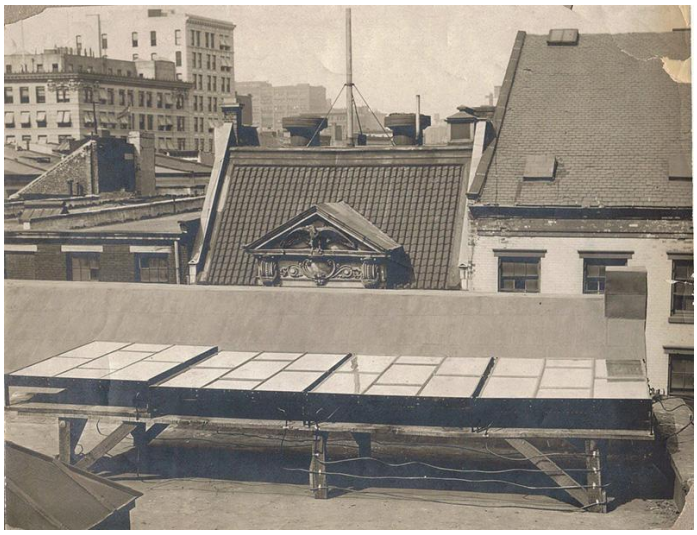

Figure 1. First solar panels installed by Charles Fritts in New York City, 1884

Solar cells were first put to practical use in 1958 when solar cells fabricated by Hoffman Electronics were used as power source for Vanguard satellite of the United States space programme [5], and solar cells were widely used in satellites afterwards. Since then, the use of solar cells has expended greatly, with it being the third most important renewable energy source after hydropower and wind power in the early 2010s and potential to overtake wind power in terms of installed power generation capacity [1].

Types of solar cells

Other than silicon solar cells, other types of solar cells have been developed. The different types of solar cells are usually grouped into three categories: first generation, second generation and third generation solar cells [7]. Silicon solar cells, or more specifically crystalline silicon wafer solar cells, are grouped in the first-generation solar cells. It is the oldest solar cells technology and currently the most widely used solar cells with around 95% market share in 2017 [8], due to silicon being cheap and abundant [7], and also due to efficient supply chain, standardisation and strongly reduced profit margins, which help to reduce the price of the solar cells [8]. There are two types of crystalline silicon wafer used in solar cells: monocrystalline silicon and polycrystalline silicon. Monocrystalline silicon wafer solar cells are fabricated through Czochralski process, which is an expensive and complicated process to produce single silicon crystal without any crystal grains. The more widely used ones are the polycrystalline silicon wafer solar cells due to their ease of fabrication and lower cost, but with the trade-off of lower efficiency [9].

The second-generation solar cells consist of thin film solar cells designed to be an alternative to crystalline silicon solar cells and achieving acceptable efficiencies with lowered costs. Some early examples are amorphous silicon (a-Si) solar cells, first prepared in 1972 by David Carlson and Christopher Wronski from RCA Laboratories with 1.1% efficiency, and the development of copper sulphide and cadmium sulphide thin film solar cells with efficiency over 10% by researchers at University of Delaware in 1980 [4].

Amorphous (a-Si) solar cells are attractive because it can be produced using low processing temperature and lower amount of energy, with possibilities of using low-cost polymer and other flexible substrates. Therefore, a-Si solar cell is comparatively cheaper than the crystalline silicon solar cells, but with caveat of lower efficiency at around 4-8 % [9]. Other promising materials used in second-generation solar cells are copper-indium-gallium diselenide (CIGS) thin film, which can reach efficiency of 20 % [9], and cadmium-telluride (CdTe) thin film. But second-generation solar cells are not as used as widely as the first-generation

solar cells due to technological problems and module stability [10].

The third generation of solar cells consists of diverse cell types such as dye-sensitised solar cells (DSSCs), organic solar cells, perovskite cells and quantum dot cells [7]. Quantum dot cells are developed with aim for the nanocrystals semiconductor material to replace bulk state semiconductor material such as Si, CdTe or CIGS [9]. Organic solar cells are solar cells with organic polymers as semiconductor materials. Thin layers of polymers consist of mixture of amorphous and crystalline regions, which can have major role in the carrier transport in the bulk material [7]. Perovskite cells are solar cells consisting of perovskite material with formula of ABX_3, where A represents a protonated amino group, B stands for Pb or Sn, and X stands for halides [11]. They have low bulk-trap density, ambipolar charge transport, wide band absorption and long charge carrier diffusion lengths, making them a highly promising candidate for solar cells as proposed by Akinoglu and team [7] with highest efficiency of 22% have been achieved, but with major drawback such as stability and reproducibility issues that prevents them from being commercialised widely [11]. DSSC was first successfully developed by Brian O'Regan and Michael Grätzel [12], with efficiency of around 7% under direct sunlight by utilising a nanoporous titanium dioxide (TiO_2) as thin layer semiconductor material with dye molecules adsorbed on its surface to absorb photons and converting it into electricity.

O'Regan and Grätzel's DSSC

The successful development of efficient DSSC by was spearheaded by Michael Grätzel and Brian O'Regan from 1988 until 1991 [12]. Although there were multiple attempts for creating DSSC previously, but all of it were of very low efficiency [13]. Previous attempts only achieved low absorption of incident monochromatic light via a layer of sensitiser on smooth surface, and using several layers of sensitiser to overcome the problem was unsuccessful.

There were also attempts to increase the dye molecules that could be adsorbed on the semiconductor surface via increasing the roughness of the semiconductor, but the conversion efficiency of the cells remains under 1%. Furthermore, the dye previously used were lacking in stability. Gratzel and O'Regan's device consisted of TiO_2 nanoparticles with average size of 15 nm deposited on a conducting glass surface to form a thin film with thickness of 10 μm as the photoanode, while the dye they used was a trimeric ruthenium complex, with iodide/triiodide redox mediator. The absorption spectrum of the thin film sensitised with the dye was redshifted and it achieved almost 100 % absorption of light in the visible spectrum under 550 nm. The conversion efficiency of the cells at one tenth and full sunlight were at 7.9 % and 7.12 % respectively, with the performance increasing to 12 % under diffuse sunlight. The cell performance was also considerably more stable compared with previous cells, with less than 10 % change in photocurrent produced by the cell after two months of testing [13]. The DSSC as invented by O'Regan and Grätzel was a significant development in DSSC history, and their device is still being studied and continuously improved by other researchers to this day.

Advantages of DSSCs

DSSCs have been gaining interest from researchers because they offer several advantages compared to the conventional silicon crystalline solar cells that are widely used today. Among the advantages of DSSCs is their capability to perform well under low light condition, as showcased by O'Regan and Grätzel in 1991 [12] when they obtained DSSC efficiency of 12% under diffuse sunlight compared to DSSC efficiency of 7.1-7.9% under direct sunlight. Unlike the silicon wafer solar cells, the performance of DSSCs is less affected by light intensity and the angle of incident, which makes DSSCs suitable for light harvesting under indoor lighting and low-level outdoor lighting [14]. Thus, DSSCs have potential for widespread application in portable electronics capable of self-powering without the need for power source from batteries, which is crucial as the Internet of Things (IOT) becoming more popular [15].

Another advantage is that DSSCs can possibly be offered with various design options, such as varying their transparency and colours. They also can be flexible and lightweight [16], which makes them

suitable for applications in small, portable electronics for indoor use, and also for application through integration in buildings and automobiles, thus helping to reduce their energy use carbon footprint. Furthermore, DSSCs are simpler and less energy intensive to produce compared to the conventional silicon wafer solar cell, which makes them possibly more practical and cost-efficient for large scale production [17]. With low energy use for DSSCs production, the energy payback time for DSSCs can be achieved in less than a year [16], which is much shorter than energy payback time for silicon solar cells [18]. Through molecular engineering of the dyes used in DSSCs, the optical properties of DSSCs can be transformed.

Challenges for widespread adoption of DSSCs

There are still several challenges that need to be overcome or mitigated before the DSSCs can be applied in large scale like the silicon crystalline solar cell. One of them is the relatively low efficiency of DSSCs. The highest cell performance achieved with DSSC is 14.3% [19]. Meanwhile, the efficiency of conventional crystalline silicon solar cells used are usually around 14-18% [10]. Other challenge is the price-competitiveness of DSSCs. At the time the first efficient DSSC was invented by Gratzel and O'Regan in 1991, the price of silicon crystalline solar cells was still high. But now, as of 2022, their price has dropped tremendously [7]. In fact, the cost effectiveness of using silicon solar cells for electrical generation have become higher than producing electricity at power plants using coal, oil or natural gas, which could possibly reduce interest for research in to improve efficiency of alternative solar cells such as DSSCs.

Commercialisation of DSSC

As for 2020, there has been penetration of DSSCs in the solar cell market, but the global solar cell market is still dominated with silicon wafer solar cell, with around 95 % market share [20]. The applications for DSSCs are as shown in Figure 2 below:

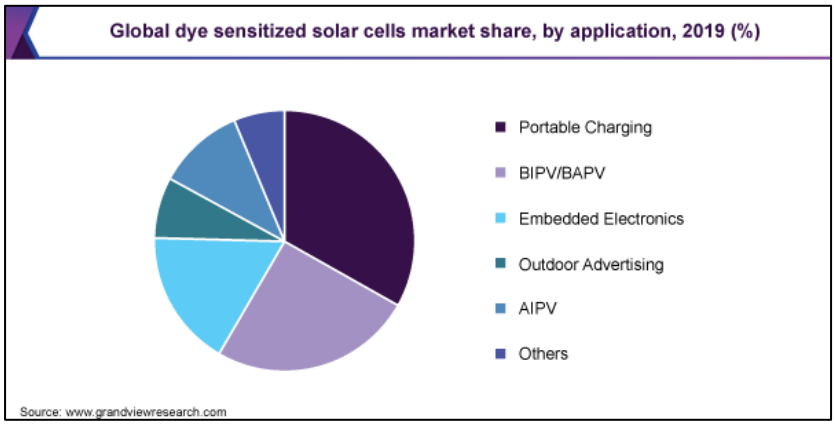

Figure 2. Global market share of DSSCs by application as for 2020

The value of the global DSSCs market is at USD 90.5 million in 2019 [21]. It was forecasted to continue growing in the future, due to the increased concerns about energy sustainability and impacts of the energy generation from non-renewable resources on the environment. DSSCs are mainly used in portable charging, building integrated photovoltaics/building applied photovoltaics (BIPV/BAPV), embedded electronics, outdoor advertising and automobile integrated photovoltaics (AIPV). Although DSSCs can have hard time to compete against the dominance of silicon based solar cells in large scale, outdoor application, but it has significant potential for indoor use [22] due to its excellent performance under low-light condition, variable design in their colour and transparency, lightweight and flexible material.

There are a number of companies involved in the DSSCs market. One of the notable companies is G24 Power, previously known as G24i. It was the first company to

produce DSSC for commercial application, with their products being used in backpacks and bags [23]. Their DSSC products are marketed under the brand name GCell (gcell.com). The next company is 3GSolar. Their products are advertised to eliminate the need for constant battery changing and charging in wireless electronic devices for the lifetime of the devices (3gsolar.com). Another player in the DSSC market is Solaronix. The company is deeply involved in the market because it not only offers DSSC kits, but it also offers the materials needed for making DSSC, such as the electrolytes, dyes, and TiO_2 paste for photoanode [24].

Main components of DSSC

A typical DSSC consists of four main components:

a) Electrolyte/redox mediator
b) Counter electrode
c) Photoanode/working electrode
d) Metal oxide nanoparticles (commonly TiO_2) with dyes molecules adsorbed on its surface

A diagram of typical DSSC as coined by Nazeeruddin [17] is depicted in Figure 3 below.

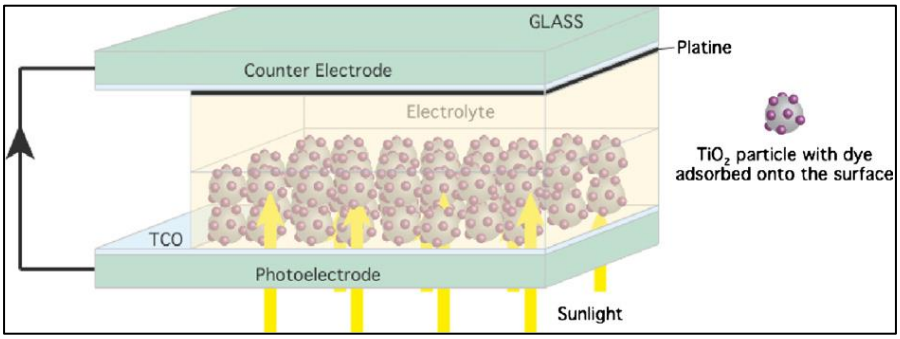

Figure 3. Schematic diagram of a DSSC

Electrolyte/redox mediator

The function of electrolyte is providing medium for the flow of electrons from the counter electrode (cathode) to the dye molecules adsorbed on the semiconductor layer (usually TiO_2) surface at the photoanode. There are several types of electrolytes used in DSSC, which are:

a) Liquid electrolyte, example is I^-/I_3^- electrolyte
b) Solid state electrolyte, example is spiro-OMeTAD
c) Quasi solid state electrolyte, example is I^-/I_3^- absorbed in PET matrix

The most commonly used type of electrolyte in DSSC is liquid electrolyte. A good liquid electrolyte needs to be chemically stable, has low viscosity to enhance electron transport capability, capable of good dissolution of the redox couple but does not significantly dissolve the dye and the semiconductor layer [16]. Among the liquid electrolytes, I^-/I_3^- electrolyte is commonly used because it demonstrated favourable kinetics. The I_3^- reacted slower with the electrons in TiO_2 than the time needed for electron injection from the dye into TiO_2 conduction band, while I^- reacts more favourably with the oxidised dye molecules than the injected electrons in TiO_2 [25]. Thus, recombination reaction could be slowed, and high efficiency can be achieved.

Other liquid electrolytes have been used in DSSC, such as Br^-/Br_3^-, $SCN^-/(SCN)_2$, $SeCN^-/(SeCN)_3^-$, $Fe(CN)_6^{3-}$ /$Fe(CN)_6^{4-}$ and Co(II)/Co(III) complex. Another type of liquid electrolyte that has been developed is ionic liquid electrolyte. It is basically a room temperature molten salt, unlike earlier liquid electrolytes in which the redox couples are dissolved in an organic solvent. But, ionic liquid electrolytes can and still have some additional solvent in it, albeit in lower amount. The salts used consists of organic cationic parts, such as alkylimidazolium, trialkylsulfonium, phosphonium and tetraalkylammonium, while for the anionic parts, halides such as iodide, and other types of anions such as PF_6^-, BF_4^- and CF_3COO^- were used [26]. Ionic liquid

electrolytes' advantage compared to the earlier liquid electrolytes is their low volatility, which ensure the electrolyte possess higher stability, but in turn, they usually have low viscosity, and thus low ion mobility [27].

The main drawback with most liquid electrolyte is their long-term stability, due to the volatility of the solvent used and prone to leakage. Thus, solid state electrolyte has been developed to overcome the issues. Solid state electrolyte consists of hole transporting materials (HTM) that function via the movement of positive charge between neighbouring molecules, as opposed to liquid electrolyte where charge transport is due to movement of redox mediators [16]. The most successful solid-state electrolyte that has been developed was the organic molecule spiro-OMeTAD. It is capable of achieving incident photon to electron conversion efficiency (IPCE) of 33%, originally yielding efficiency of 0.74 % [28]. However, the efficiency of solid-state electrolytes is still lacking compared to liquid electrolytes, mainly due to the very fast recombination between electrons in TiO_2 with holes in the HTM [29], and also the poor contact between the dye and electrolytes [12].

Another alternative electrolyte that has been developed is quasi solid-state electrolyte that can show the properties of liquid and solid simultaneously. The advantages of quasi solid-state electrolyte are their stability from leakage and vaporization of the electrolyte, close interfacial contact with the TiO_2, and relatively good ambient ionic conductivity [25]. An example of quasi solid-state electrolyte is from the work of Sun and co-workers [30], where they used polyethylene terephthalate to act as matrix for the iodide/triiodide liquid electrolyte by absorbing the liquid electrolyte to become quasi solid-state electrolyte.

Counter electrode

Counter electrode accepts electrons from the external circuit and utilise it to catalyse redox reactions in the electrolyte. A counter electrode consists of a conductive substrate (usually glass) that is coated with a thin layer of catalytic material. Among the properties for a good counter electrode are high catalytic activity, good conductivity, high reflectivity, large and porous surface area, suitable thickness of the coated catalytic layer, good stability against degradation, compatible energy level with the potential of the redox couple electrolyte, and good adhesion of the catalytic layer with conducting substrate [31].

The conductive substrate is coated with catalytic materials to reduce the charge transfer overpotential by increasing the speed of the reaction. Charge transfer overpotential originates from the electrolyte/counter electrode interface, and high charge transfer overpotential causes the output voltage of the DSSC to be significantly reduced. The magnitude of the charge transfer overpotential is dependent upon the electrocatalytic properties of the counter electrode surface towards mediator reduction [32], and coating the surface of the conducting substrate with catalytic material helps to increase conductivity and improve electrocatalytic activity of the counter electrode [33].

As for the catalytic layer, the most commonly used material is platinum. It was used in the pioneering work of O'Regan and Grätzel DSSC in 1991. It is widely used because of its ideal properties such as high catalytic activity, high electrical conductivity, good stability and high reflectivity [33]. In the DSSC fabricated by O'Regan and Grätzel, the conducting substrate used was the FTO coated glass, but it has high charge transfer resistance in iodide/triiodide electrolyte, and its surface is also very unconducive for the reduction of triiodide to iodide. Due to the ideal properties of platinum, it was chosen as the catalytic layer for the counter electrode of DSSC, and it has been popular since 1991 [33].

The platinum layer's thickness on the DSSC may significantly affect its performance. Nearly two decades ago Fang and team found out that the different layer thickness ranged from 25 nm to 415 nm did not prominently affect the charge transfer resistance at the electrolyte-counter electrode interface. They also discovered that increasing the thickness from 2 nm to 415 nm decreases the sheet resistance of the counter electrode, but no significant difference was observed in the DSSC performance. Thus, 2 nm of platinum layer

was sufficient for the DSSC to obtain good efficiency [34].

Other factors, such as the size and shape of the platinum particles also affect the performance of the DSSC. Platinum nanoparticles perform better than bulk platinum in DSSC due to their large surface area, high electrical conductivity, low charge transport resistance, good resistance against corrosion, and high transmittance [35]. Platinum nanoparticles with variety of shapes have been developed to increase their surface area and improve their properties in counter electrode.

One example is platinum nanocup developed by Jeong and co-workers [36]. In their work, they synthesised two platinum nanocup in different sizes and compared their performance with planar platinum for the counter electrode. The platinum nanocups have larger surface area than the planar platinum, so more sites are available for catalytic process on the platinum nanocup surface. Thus, it enables more electrochemical reduction by reducing the charge-transfer resistance at the counter electrode/electrolyte interface. The lowering of internal resistances of RCT helps in increasing the fill factor and short circuit current of the DSSC. The DSSC with the platinum nanocup array with a diameter of 300 nm at a 400 nm pitch size showed a power conversion efficiency of 9.75%, which is 24% higher than the 7.87% power conversion efficiency of DSSC with the planar platinum.

Although platinum has ideal properties for counter electrode, it also has several disadvantages, such as its high price, low abundance, and weak corrosion resistance against the commonly used iodide/triiodide electrolytes, so many researchers have been developing alternatives material for platinum in counter electrode. One of the alternative materials is carbon. It possesses suitable properties for counter electrode material, such as good catalytic activity, high conductivity, large and porous surface area, and chemical resistance against electrolyte and dye solution. More importantly, it is also available abundantly on earth and also cheaper to obtain than platinum, so it is a promising material [31]. There are different types of carbon materials used for counter electrode materials, examples are graphene, carbon nanotubes, carbon nanofibers, activated carbon, graphite, and carbon black [33].

Photoanode/working electrode

Photoanode, also called as working electrode, receives electrons from the excited dye molecules, which then would flow to the counter electrode through external circuit. A photoanode consists of transparent conducting substrate deposited with a layer of metal oxide semiconductor material. The conducting substrate must be high transparency for the dye molecule to be able to absorb light, and low electrical resistivity to minimise energy losses and facilitate electron transport process. The transparent conducting substrate is usually made of glass substrate for physical support, with a layer of transparent conducting oxide (TCO) on it. Examples of TCO materials are fluorine doped tin oxide (FTO), indium doped tin oxide (ITO), aluminium doped zinc oxide (AZO) and antimony doped tin oxide (ATO).

Among them, FTO is the most widely used TCO because of their suitable properties such as good light transmittance, good electrical conductivity, good adhesion with the glass substrate, high Mohs hardness, good resistance against corrosion, chemically stable, and can resist heat up to 600 °C [33]. The high heat resistance is important because the catalytic layer deposited on the conductive glass substrate needs to be solidified by calcination at high temperature. Other than glass, polymers and metals also have been used for the physical support, with polymers such as polyethylene terephthalate and polyethylene naphthalate, and metals such as stainless steel, titanium and tungsten.

For the semiconductor metal oxide layer, it should have several properties to make it an ideal material [37]:

a) Large surface area so more dye can be adsorbed on it
b) Facilitates fast electron transport from the excited dye to the external circuit
c) Optimum pore size for good diffusion of dye and electrolyte on it
d) High resistance against photo-corrosion
e) Capable of absorbing and scattering light to facilitate the dye functioning efficiently

f) Good electron acceptor
g) Good interfacial contact with the dye molecules and also the TCO layer on the substrate

The semiconductor material also must have band-gap of more than 3 eV [30]. The higher the band-gap, the UV light absorbed from the sun would be lower, thus reducing reactive holes formed in the semiconductor when it is excited by the sunlight. The reactive holes are undesirable because they can disturb and damage the organic compounds in DSSC, such as the dye molecules, via oxidation reaction [28]. Examples of materials that have been used for photoanode are titanium dioxide (TiO_2), zinc oxide (ZnO), tin oxide (SnO_2) and zinc stannate (Zn_2SnO_4). Their band-gaps are as depicted in Figure 2.4 below as proposed by team of Gong in 2012 [25].

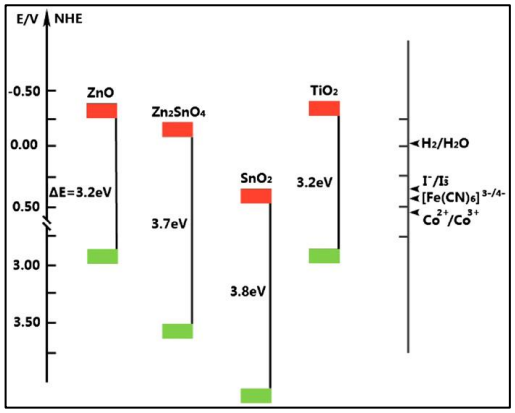

Figure 4. Band-gaps of materials for photoanode

The most widely used material for photoanode is TiO_2. In their 1991 work, O'Regan and Grätzel pioneered the use of it in DSSC, and to this day, it is still popular due to its low cost, easy availability and non-toxic [12]. It usually exists in three crystalline forms, which are rutile, anatase and brookite, with band-gaps of 3.05 eV, 3.20 eV and 3.28 eV, respectively [31]. Among the three, anatase-form TiO_2 is the most preferred form for use in DSSC. In comparison to the anatase-form TiO_2, rutile-form has smaller band-gap. DSSC using the rutile-form TiO_2 has lower photocurrent due to the lower amount of dye molecules adsorbed on the TiO_2 film surface, which is because of their smaller surface area than anatase-form TiO_2. In addition, electron transport is also slower in the rutile form than in the anatase form due to differences in the extent of inter-particle connectivity associated with the particle packing density [38]. As for the brookite-form TiO_2, although it has wider band-gap than anatase-form TiO_2, the brookite-form has lower dye loading due smaller surface area for the dye on the brookite surface compared to anatase surface. The conduction band edge in brookite-form is similar or below that of the anatase-form photoanode. Undesirable recombination side reaction is lower in brookite cell, thus enabling it to obtain higher open circuit voltage than anatase cell. But, the electron transport is significantly slower in brookite cell compared to the anatase cell due to its lower electrical conductivity, thus tremendously reducing its electron collection efficiency compared to anatase cell [39].

Other than TiO_2, other photoanode materials that have been frequently used are ZnO. In fact, ZnO has been studied for semiconductor use in DSSC since 1972, way earlier than TiO_2 [40]. Although it has been overtaken by TiO_2, ZnO can still be considered as a suitable alternative to anatase-form TiO_2, due to their nearly similar conduction band edge and same band-gap, and higher electron mobility in ZnO than TiO_2 [25], which facilities electron transportation by decreasing the recombination loss [40]. It is also relatively easy to synthesise highly crystalline ZnO (wurtzite-form) with different morphologies, such as nanoparticles, nanowires, nanorods, nanotubes, tetrapods, nanoflowers, nanosheets, and branched nanostructures [16]. However, ZnO have several disadvantages such as low carrier concentration, low fill factor, poor stability in acidic dyes and slow electron injection kinetics [41]. The highest DSSC efficiency achieved using ZnO photoanode is 8.03% [42], which is still low compared to the highest DSSC efficiency achieved with TiO_2 photoanode at 14.3% [19]. Even with many other metal oxide alternatives, TiO_2 is still the superior material of choice for photoanode.

The performance of TiO_2 and any other photoanode material is mainly affected by three factors, which are the size/surface area of the particles, the morphology/shape of the particles, and the

composition/purity of the photoanode material [31]. Nanoparticle-sized material is better than bulk size material, due to the higher surface area provided by the nanoparticles, which enable it to adsorb more dye molecules on it. O'Regan and Grätzel achieved high efficiency DSSC by using TiO_2 nanoparticles with average size of 15 nm. But smaller particle size does not guarantee better performance, [43]. They compared the performance of several TiO_2 nanoparticles films, and they observed that the films with larger particle size achieved higher short-circuit current density and better conversion efficiency. They concluded that even though the surface area of the smaller particles is larger than of the bigger particles, the bigger particles may have better dye adsorption properties by providing easier access for the dyes to its surface, resulting in a higher number of electrons and holes produced. The size distribution range of the nanoparticles also plays a role. In a study by Dhungel and Park [44], TiO_2 film with smaller size distribution range have poor interconnection between the nanoparticles, so its porosity is increased, which in turn increased the area available for the adsorption of dye after sintering. So, the size of the nanoparticles, their size distribution and surface area need to be optimised to ensure higher dye adsorption on the surface.

The next main factor is morphology or shape of the particles. There have been numerous studies on tuning the morphology of the TiO_2 nanoparticles to improve their performance. A study by Wang et al. [45] compared the performance between monolayer, double layer and multilayer TiO_2 photoanode. Small nanoparticles have large surface area, thus capable of adsorbing more dyes than large particles, but they have poorer light scattering ability than large particles. Poor light scattering ability leads to weaker absorbance of longer wavelength red light.

To overcome that, Wang and co-workers [45] have developed a multilayer photoanode structure incorporating nanoparticles layer (23 nm), followed by nanoparticles-scattering particles (50 nm) mixture layer and nanoparticles-scattering particles (100 nm) mixture layer, and lastly with scattering particles (100 nm) layer, with purpose to balance the surface area for dye adsorption with light scattering ability. Their multilayer cells achieved higher light harvesting efficiency (10.2%) than the monolayer and double layer cells. However, the mesoporous nanostructure still suffers from low electrical conductivity and the pores facilitate recombination reactions to occur. Thus, many researchers have been focused on developing new nanostructured photoanode material to obtain high conductivity and also high dye loading. Examples are nanowires, nanotubes and hollow spheres [37].

The last main factor is composition/purity of the photoanode material. Electronic band structure of semiconductors can be altered by substitutional doping, which is done by substituting some of the semiconductor atoms with different atoms of similar atomic radius [46]. TiO_2 photoanode has been doped with several materials, such as copper [47], sulfur [48], and calcium [49], and all of them successfully obtained higher cell efficiency compared to the undoped TiO_2 photoanode. Other than doping, semiconductor material has been used as composite within combination with other component, in which the mixture can be in the form of core-shell or layered frameworks [46]. Examples of TiO_2 composites are TiO_2-ZnO composite [50], TiO_2-SnO_2 composite [51], and TiO_2 nanorod-nanoparticle composite [52].

Dye/photosensitiser

Dye, also called as photosensitiser, absorbs light, resulting in excited electron which is then injected into the conduction band of the metal oxide semiconductor layer (usually TiO_2) in photoanode. The oxidised dye would then be reduced to its normal state by receiving electron from the electrolyte. The dyes used can be either metal based dyes, most commonly using ruthenium (Ru) metal, or metal-free organic dyes, which are either synthetic dyes or natural dyes extracted from plants. A good dye is vital to achieve DSSC with high conversion efficiency. Characteristics of a good dye are as follows [16]:

a) The dye should strongly absorb wavelength ranging from the visible region to the near-infrared region
b) The dye should have anchoring groups such as carboxylic acid (COOH), phosphonic acid

(H_2PO_3) or sulfonic acid (SO_3H) groups for it to be able to bind onto the semiconductor surface

c) The excited state level of the dye should be higher in energy than the conduction band edge of n-type semiconductor, so that an efficient electron transfer process between the excited dye and conduction band (CB) of the semiconductor can take place

d) For dye regeneration, the oxidized state level of the dye must be more positive than the redox potential of electrolyte

e) Unfavourable dye aggregation on the semiconductor surface should be avoided through optimization of the molecular structure of the dye or by addition of co-adsorbers that prevent aggregation

f) The dye should be stable against degradation by light, in addition to possessing electrochemical and thermal stability

By having a wide and intense absorption spectrum both the visible and the near-IR, the dye can absorb lighter, which in turn can lead to more photocurrents being produced [53]. Approximately 46% of total energy from sunlight is in the infrared region [1], which is only weakly absorbed by the commonly used crystalline silicon solar cell. The weak absorbance is compensated by using relatively thick silicon layer (~100 μm), but this led to increased material cost and some losses in power conversion efficiency due to recombination reaction [54]. Thus, DSSC has an advantage over crystalline silicon solar cell due to its cheaper material, much thinner structure (~20 μm), and higher potential capability to absorb light in the near-infrared region. And by utilising strong light absorbing dye (i.e., high molar absorption coefficient), the semiconductor layer can be made thinner, thus reducing the material used and also minimising the unwanted recombination reactions from occurring [55].

Anchoring groups bind the dye molecules to the semiconductor metal oxide surface, with carboxylic acid, cyanoacrylic acid and phosphonic acid being among the most frequently used anchoring groups [56-57]. They bind to the metal oxide by reacting with the hydroxyl group on it to form ester linkage. Anchoring groups can profoundly affect the operating parameters of DSSC, such as light absorption, molecular orbital distribution, frontier orbital energy levels, band structures of the photoanode, electron transport between the dye and photoanode, charge recombination, and overall solar-to-electron conversion efficiencies of the DSSC [57].

In order to ensure efficient charge injection, the energy level of lowest unoccupied molecular orbital (LUMO) of the dye molecule should be slightly above (i.e. more negative) the conduction band (CB) edge of the semiconductor metal oxide, while the energy level of highest occupied molecular orbital (HOMO) should be lower (i.e. more positive) than the redox potential of redox mediator. The difference between E_{LUMO} and E_{CB} acts as an enthalpic driving force for electron injection from the excited dye to the semiconductor by ensuring the injection process is kinetically favourable. And by having the dye's highest occupied molecular orbital (HOMO) to be below the electrolyte redox potential, this induces the process of electron transfer to the excited dye, which regenerates the dye in its ground state. This separates the charges and is the major mechanism for charge separation in the DSSC [58].

Dye aggregation on semiconductor surface is generally unwanted because it can cause low conversion efficiency of the DSSC via reduction of electron injection yield from the dyes to the CB of semiconductor due to intermolecular energy transfer [59]. The common structure is that the dyes would form a homogenous monolayer on the semiconductor surface with relatively uniform spacing between the dye molecules. There are several ways in which the dye molecules could aggregate either laterally or longitudinally on the semiconductor surface as depicted in Figure 2.5. Longitudinally, the dye molecules could clump together haphazardly, resulting in unequal spacing between them. Another way is the dye molecules also could cluster too close to each other, thus forming an aggregate layer. While for lateral aggregation, instead of being adsorbed on the semiconductor surface, a dye molecule could interact with the tip of another dye molecule that is adsorbed on the semiconductor surface [57] (Figure 5).

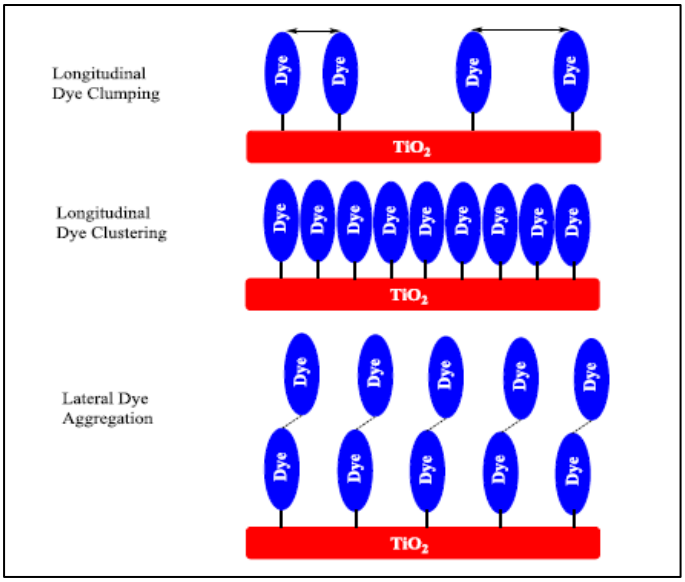

Figure 5. The possible dye molecules' arrangement on TiO_2 surface

The methods that have been used to prevent dye aggregation were tuning the molecular design of the dye molecule, using co-adsorbent in tandem with the dye, or using a different dye compound as co-sensitizer. The dye can become degraded due to seepage of moisture or oxygen in DSSC, and exposure to UV light in sunlight, which could directly excite the semiconductor and may lead to irreversible oxidation of the dye [60]. Under illumination, degradation can occur during the excited state dye or the oxidised state dye. The electron injection from excited dye state to the CB is extremely fast, so light induced degradation is thought to mostly happen at the oxidised state dye. For widespread DSSC utilisation to be become viable, other than improving the power conversion efficiency, it is vital to also increase the stability of DSSC. One way to achieve that is by using a dye possessing good light, electrochemical, and thermal stability, so the dye is capable of operating consistently without significant degradation and performance loss for at least for 20 years [55].

As mentioned previously, the three dye types that have been used in DSSC are either metal based dyes, most commonly using ruthenium (Ru) metal, metal-free synthetic organic dyes, or natural dyes extracted from plants. Metal based dyes have been frequently studied for DSSC application because of their broad absorption spectra and favourable photovoltaic properties. The structure of metal-based dye generally consists of complex with a central metal ion and auxiliary ligands with one or more anchoring group. The metal complex is able to absorb light in the visible spectrum of sunlight due to metal to ligand charge transfer (MLCT) process. Substituents such as alkyl, aryl or heterocyclic alkyl can be used to modify the photophysical and electrochemical properties of the ligands, and thus helps to improve the DSSC performance via tuning the energy levels of the MLCT states, optimisation of electron injection process and improvement of dye regeneration kinetics [16].

Among the metal-based dyes, Ru based dyes have the best performance record, with their broad absorption spectrum, optimum excited and ground state energy levels, relatively long excited-state lifetime, and good electrochemical stability [16]. The first DSSC with high efficiency developed by O'Brian and Grätzel in 1991. They used ruthenium complex dye. In 1993, Nazeeruddin et al. managed to fabricate DSSC with conversion efficiency of 10% by using cis-RuL_2-$(NCS)_2$ dye that incorporates 2,2'-bipyridyl-4,4'-dicarboxylic acid as ligands, with codename N3 dye. It was the first time a DSSC device managed to achieve conversion efficiency of 10 % and above [16].

N3 dye possess superb qualities, such as broad visible light absorption spectrum with threshold up to 800 nm, relatively long excited state lifetime, and excellent adsorption to the TiO_2 semiconductor surface via four carboxylates anchoring groups that are linked to the two bipyridyl moieties. The four carboxylates anchoring groups also facilitates improved electronic coupling between the charge-transfer excited state and the conduction band wave function manifold of the semiconductor [61]. Later on, the team studied the effects of protonation on the several Ru complex dyes also with 2,2‘-bipyridyl-4,4‘-dicarboxylic acid as ligands. One of the synthesised dyes, the doubly protonated $(Bu_4N)_2[Ru(dcbpyH)_2(NCS)_2]$ with codename N719, exhibited a higher power conversion efficiency than the other dyes [62]. Since then, the N3 and N719 dyes are considered as reference dyes for DSSC, and are also used by other researchers as template for designing other Ru based dyes by modifying its ligand moieties [16].

Other than Ru, other metals such as osmium (Os), copper (Cu), and platinum (Pt) have been investigated for their potential application in metal complex dye. Os complex dyes have been studied because it exhibited excellent photosensitisation, with better MCLT than that of Ru complex dyes [63]. The synthesis of several Os polypyridyl complexes for comparison with Ru polypyridyl complexes, and they discovered that the Os polypyridyl complexes exhibited broadening of the light absorption and extended the spectral response of nanocrystalline TiO_2 photoelectrodes to higher wavelength values while still maintaining the same performance as Ru polypyridyl complexes [64]. However, Os based dyes suffers from poor reduction of adsorbed dyes by the iodide/triiodide redox couple due to the process being kinetically unfavourable in comparison with the charge recombination process, thus limiting its photocurrent efficiency [65-66]. Among the earliest Pt complex dyes used in DSSC were square-planar platinum(II) diamine dithiolate dyes [67], and they managed to achieve efficiency of 2.6%. Other examples of Pt complex dyes are phenothiazine-based platinum(II)–acetylide dyes developed by Siu et al. [68] and platinum(II) bis(aryleneethynylene) dyes [69]. They managed to achieve highest efficiency of 5.78% and 1.57%, respectively. Still, there are much more studies need to be done for improving the performance of non-Ru complex dyes to become comparable to Ru complex dyes.

Although Ru based dyes have excellent properties, there are several drawbacks associated with it, such as the high cost of Ru metal, non-abundant supply, and the sophisticated synthesis and purification steps [25]. Recently, metal-free organic dyes have been subject to numerous studies in hope of developing promising alternatives comparable or superior in performance to Ru based dyes. Organic dyes have several advantages over Ru and also other metal-based dyes, such as easier to synthesise and purify, lower material cost, low concern of supply limitations, higher molar absorption coefficients, and wider variety of structural design modification of the organic dyes are possible to tune their properties [59].

The usually high molar absorption coefficients of organic dyes in comparison to the metal-based dyes allows the use much thinner semiconductor layer, thereby facilitating the charge transport in the photoanode and minimising energy loss, and also improving the pore filling properties for quasi-solid-state or solid-state electrolyte in porous dye-sensitized TiO_2 films [70]. Usually, organic dyes are designed with the template of donor-π bridge-acceptor (D-π-A) structure, as shown in Figure 6 below which in this particular work carried out by Shalini et al. [55] involved D-π-A structure adsorbed on TiO_2. By adjusting the design template, it is possible to broaden the absorption spectra, shift the HOMO and LUMO energy levels, and improve the intramolecular charge separation of the organic dye [16]. When a dye absorbs light, electron is transported from the donor part through the π-bridge to the acceptor part, which is then injected into the CB of semiconductor. D-π-A structure ensures that the majority of electron transport occurs in one direction.

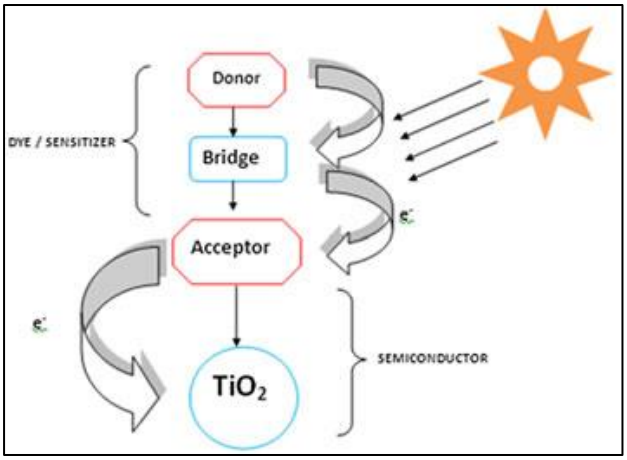

Figure 6. Schematic diagram of dye with D-π-A structure adsorbed on TiO_2

Working mechanism of DSSC

When a dye (S) is exposed to sunlight, it absorbs a photon to become photoexcited state (S*), in which an electron becomes excited and moved from HOMO to LUMO of the dye (Eq. 1). The photoexcited dye then injects an electron from its LUMO into the CB of photoanode (i.e. TiO_2), thus becoming oxidised dye (S^+) in the process (Eq. 2). The oxidised dye is then reduced to its normal state (S) by accepting electron from the redox mediator, i.e. I^- in I^-/I_3^- redox couple, thus regenerating the dye (Eq. 3). Meanwhile, the electron injected into the CB of TiO_2 travels through the interconnected TiO_2 nanoparticles and arrived at the TCO coated glass (i.e. FTO glass), and then it enters the external circuit and transported to the counter electrode (i.e. Pt-coated FTO glass), in which it reduced the I_3^- ion to regenerate I^- ion (Eq. 4) and thus completing the circuit. However, there are also other unwanted reactions that can interfere with the electron transport process, which are recombination reaction of the injected electron in the CB of semiconductor with the oxidised dye (Eq. 5), reaction of the injected electron with the electrolyte at the semiconductor/electrolyte interface, referred as dark current (Eq. 6), and also relaxation of the photoexcited dye (Eq. 7). The unwanted reactions can reduce the performance of DSSC if not mitigated or overcome. The electron cycle process is pictured in Figure 7 below as proposed by Ooyama & Harima [59].

.

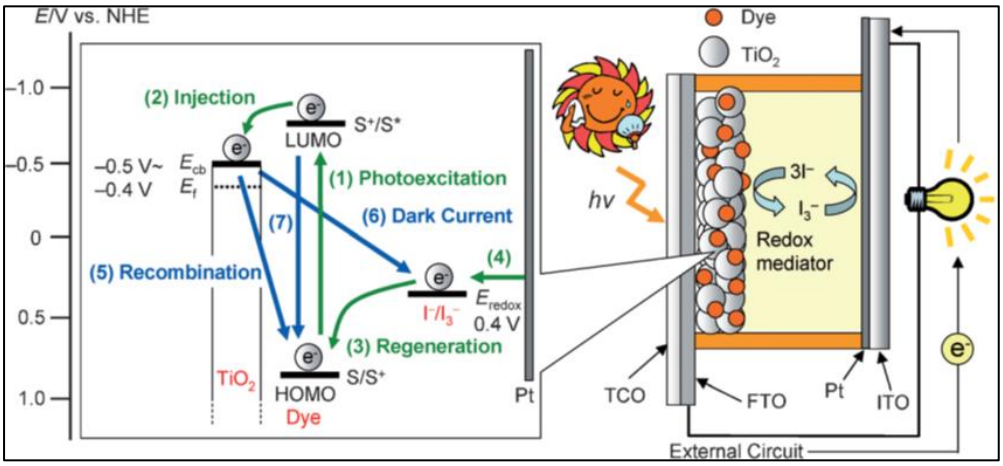

Figure 7. Electron cycle process in DSSC. The green arrows represent the processes required for the generation of photocurrents. The blue arrows represent recombination processes (electron-loss processes)

$S + photon \rightarrow S^*$ (1)

$S^* \rightarrow S^+ + e^-$ (2)

$2\ S^+ + 3\ I^- \rightarrow 2\ S + I_3^-$ (3)

$I_3^- + 2\ e^- \rightarrow 3\ I^-$ (4)

$S^+ + e^- \rightarrow S$ (5)

$I_3^- + 2\ e^- \rightarrow 3\ I^-$ (6)

$S^* \rightarrow S$ (7)

Parameters of DSSC performance

The performance of DSSC is evaluated via several parameters: incident photon to current conversion efficiency (IPCE), photocurrent/voltage curves (J/V curves), open-circuit photovoltage (V_{oc}), short circuit photocurrent density (J_{sc}), fill factor (ff), and solar energy conversion efficiency (η) [59].

IPCE, also referred as external quantum efficiency, is defined as the photocurrent density produced by the electrons flowing in the external circuit under monochromatic illumination of the cell divided by the photon flux hitting the DSSC [16]. The equation to calculate IPCE is as shown in Eq. 8:

$$\%\ \text{IPCE} = 1240\ (\text{eV nm})\frac{J_{ph}(\text{mA cm}^{-2})}{\lambda\ (\text{nm})\times I\ (\text{mW cm}^{-2})} \quad (8)$$

Where J_{ph} is the short-circuit photocurrent, density generated by monochromatic light, and λ is the wavelength while I is the intensity of the monochromatic light. IPCE provides information the monochromatic quantum efficiency of the DSSC [16].

J/V curves for DSSC is usually measured under standard AM 1.5 simulated sunlight (100 mW cm^{-2}). From the J/V curves, four values can be obtained directly: J_{sc}, V_{oc}, J_{mp} and V_{mp}, where J_{mp} and V_{mp} are the photocurrent and photovoltage at maximum power, respectively. A typical J/V curves is depicted in Figure 8 below [64].

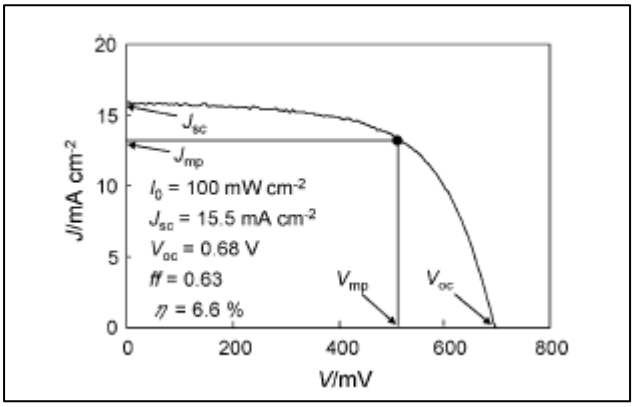

Figure 8. Typical J/V curves of a DSSC

V_{oc} is the difference in potentials between the two terminals of the cell when the circuit is being illuminated and in open state (J=0) [71]. V_{oc} can be derived from Eq. 9 shown below.

$$V_{oc} = \frac{E_{cb}}{e} + \frac{k_B T}{e}\ln\left(\frac{n}{N_{cb}}\right) - E_{redox} \quad (9)$$

Where E_{cb} is the energy level of the CB of the semiconductor, E_{redox} is the redox potential of the redox mediator, n is the number of electrons in the semiconductor, and N_{cb} is the effective density of states [59]. The maximum V_{oc} value can be defined as the difference between the E_{cb} of the semiconductor and the redox potential of redox mediator. However, the actual V_{oc} is usually lower than theoretical due to the inefficiency in electron cycle process causing losses of electrons through reactions such as recombination and dark current. The V_{oc} value could be enhanced via increasing the E_{cb} of semiconductor or lowering the E_{redox} of the redox couple [72].

J_{sc} is the photocurrent density measured when the DSSC is short-circuited, i.e. no opposing voltage that inhibits electron flow [71]. Its value is dependent upon absorption coefficient of the dye, in addition to the interaction between photoanode and the dye. To obtain

high J_{sc} value, the dyes should be capable of intense light-absorption over broad wavelength of sunlight, the electron injection process from the excited dye to the photoanode should be highly efficient, and the oxidised dye should be effectively reduced by the redox mediator [59].

Fill factor (ff) is defined as the ratio where product of current and voltage at maximum power is divided by the V_{oc} and J_{sc} as shown in Eq. 10.

$$\mathrm{ff} = \frac{J_{mp} \times V_{mp}}{J_{sc} \times V_{oc}} \quad (10)$$

The ff is determined from the J/V curve. It is essentially a comparison of how much the rectangular area defined by J_{sc} and V_{oc} is filled by rectangular area as defined by J_{mp} and V_{mp}. Thus, if the J_{mp} and V_{mp} rectangle completely fill the J_{sc} and V_{oc} rectangle, the ff value becomes unity [59]. However, the ff value is usually around 0.6 – 0.8 due to charge recombination and electron loss [71]. Electron loss are caused by the combination of series resistance in the DSSC, such as sheet resistances of the substrate and counter electrode, electron transport resistance through the photoanode, ion transport resistance, and the charge-transfer resistance at the counter electrode.

Energy conversion efficiency (η) is calculated by dividing the maximum electrical output of the DSSC divided by incident power from the sunlight as defined in Eq. 11.

$$\eta = \frac{J_{sc} \times V_{oc} \times \mathrm{ff}}{P_{in}} \quad (11)$$

Where η is the power conversion efficiency, J_{sc} is the short circuit photocurrent density, V_{oc} is the open circuit photovoltage, ff is the fill factor, and P_{in} is the incident light intensity. The incident power is usually set to the irradiance of the AM 1.5 spectrum with value of 100 mW/cm^2. From the energy conversion efficiency, it provides information about the generated power of DSSC and the light conversion into electricity and photovoltaic parameters. To improve the energy conversion efficiency, all of the components of DSSC must be optimised, with the dye as the most important component to be optimised. Numerous scientists have conducted studies to adjust their photophysical and electrochemical properties of the dyes by molecular design to improve their properties [59]. External factors, such as overall light intensity, spectral intensity distribution and temperature also affect the performance of DSSC [71].

Organic dyes as photosensitiser

There has been intense interest in research and development of organic dyes for application in DSSC due to their potential advantages against ruthenium and other metal complex dyes, such as higher molar extinction coefficient, flexibility in designing the molecules, lower material costs, and being relatively easy to prepare [59, 73]. But organic dyes also have several drawbacks compared to ruthenium complex dyes, such as narrow absorption in the visible spectrum, dye molecules aggregation, short electron lifetime in the excited state, and low stability in the long term. These drawbacks need to be overcome for organic dyes to become more efficient as photosensitisers in DSSC. The structural design of an organic dye is commonly based on the donor-pi-acceptor (D-π-A) structure as shown in Figure 9. According to Ooyama and Harima [59], an organic dye should fulfil several requirements:

a) The organic dye must have at least one anchoring group for adsorption onto the TiO_2 surface, for example –COOH group. A carboxyl group can form an ester linkage, a chelating linkage, and a bidentate bridging linkage with the TiO_2 surface to provide a strongly bound dye and good electron communication between the dye and the surface

b) For efficient electron injection from the excited dye to the CB of TiO_2, the energy level of the LUMO of the dye must be higher (more negative) than that of the CB of the TiO_2 electrode, while for efficient regeneration of the oxidized state by electron transfer from the I^3-/I^- redox couple in the electrolyte, the energy level of the HOMO of the dye must be lower (more positive) than that of the I^3-/I^- redox potential

c) Have high molar absorption coefficients over the wide range of sunlight for high light harvesting efficiency

d) The flow of electrons in the excited state of a dye should be highly unidirectional with path from the donor part to the acceptor part to provide efficient electron injection from the excited dye to TiO_2 through good electronic coupling between the LUMO of the dye and the CB of TiO_2.

e) Possess chemical stability in its photoexcited state and in the redox reactions throughout the reaction cycle so the DSSC can last longer

f) The dyes should not excessively aggregate on the TiO_2 surface because it could cause low conversion efficiency of the DSSC. Aggregated dyes reduce the electron-injection yield from the dyes to the CB of TiO_2 owing to intermolecular energy transfer between the dyes through the stacked π-bridge, especially dyes with long conjugation

g) Recombination of injected electrons with dye cations and I^{3-} ions in the electrolyte should be suppressed. Wide spatial separation between the moieties of positive charge density on the exited dye and the TiO_2 surface facilitates efficient charge separation, thus inhibiting the recombination process. Hydrophobic substituents on the dye skeleton act as barriers to prevent hydrophilic I^{3-} ions from approaching the TiO_2 surface, thereby retarding charge recombination.

D-π-A dyes consisting of electron-donating and electron–accepting groups linked through π-conjugated bridges featuring broad and intense absorption spectrum are expected to be one of the most promising classes of organic sensitizers that meet the above requirements, because D-π-A structure offers flexible designs that make it possible to obtain desirable dye properties with molecular engineering for various designated function of interests.

D-π-A dye design

As mentioned previously, the D-π-A structure consists of three parts, which are the donor part (D), π-bridge, and acceptor part (A), with donor part conjugated with the acceptor part though the π-bridge. Requirements a) to c) can be fulfilled by adjusting the photophysical and electrochemical properties of the dyes via the inclusion of electron-donating and electron-accepting groups onto the chromophore skeleton and extending the length of π-conjugation, which causes shift in the energy levels of the HOMOs and LUMOs [59]. By increasing the electron-donating ability of the donor part and electron-accepting ability of the acceptor part, the energy gaps between the HOMO and LUMO are reduced, thus resulting in redshifting of the absorption peaks. So, the dyes can absorb more sunlight in the visible region. Redshifting is vital because compared with metal complex dyes, organic dyes exhibited sharp and narrow absorption bands in the visible region, which impairs light-harvesting capabilities [75].

For requirements d)–f), they should be fulfilled through the introduction of sterically hindered substituents, such as hydrophobic long alkyl chains and aromatic units, onto the chromophore skeleton [59]. One of the main drawbacks of these D-π-A dyes is the formation of strong π-stacked aggregates between dye molecules on TiO_2 surfaces, which tends to reduce electron-injection yields from the dyes to the CB of TiO_2, due to intermolecular energy transfer between dyes. The sterically hindered substituents (bulky groups) help to prevent the aggregation of dye molecules on TiO_2 surfaces by inhibiting the π-π stacking between the dyes, and also prevent the ions in electrolyte from approaching the TiO_2 surface, thus reducing the electron recombination between the electrolyte ions and electrons in TiO_2 [76].

Utilisation of mixed moieties of D-π-A system as dyes for DSSC

In this section, several selected prior studies involving application of different selected mixed moieties featuring numerous substructures of D-π-A system in DSSCs have been focused, reviewed and discussed in relation to the scope of mixed moieties system. Thorough discussion on their characteristics and

molecular build-up are presented in respect to the unique highlights on their functionalities and performances.

Acetylene

The moiety of acetylene has been known over the years as active materials in numerous applications, synthesised in recent decades via Sonogashira cross coupling reaction [77-78]. Over a decade ago, Song et al. [79] had synthesised four dyes with triphenylamine as donor part, cyanoacrylic or carboxylic acid as acceptor part, with phenylacetylene moiety as linker. They varied the structure of the phenylacetylene linker part and the acceptor part while keeping the donor part unchanged (Figure 9).

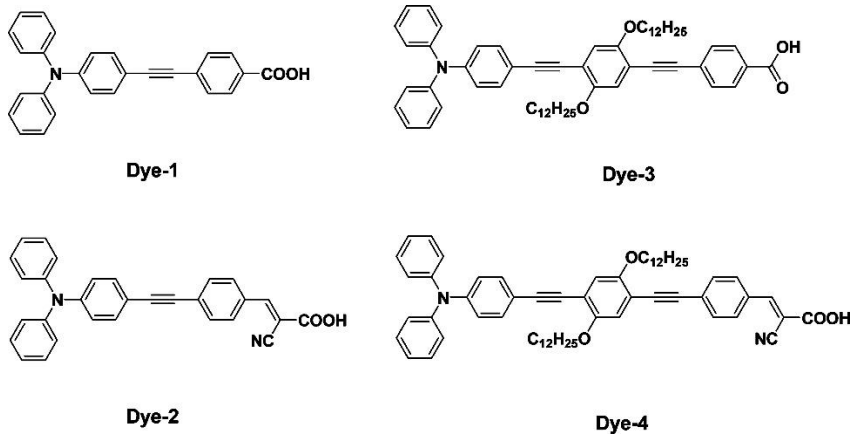

Figure 9. Structures of dyes bearing four dyes with triphenylamine as donor part, cyanoacrylic or carboxylic acid as acceptor part, with phenylacetylene moiety as linker

In recent years some alternatives have been proposed involving rather similar motifs and expected to behave fairly equal as acetylenes involving thiourea [80] and chalcone [81] derivatives with the focus in optoelectronics interests. The properties of the dyes and their DSSC performance were compared with that of the reference Ru complex N719 dye. In general, Dye-3 and Dye-4 with longer conjugation length of the double phenylacetylene moiety exhibited red-shifting in their absorption spectrum compared to the Dye-1 and Dye-2 with only one phenylacetylene moiety. It is also almost the same with their emission spectrum, except that Dye-2 and Dye-4 with cyanoacrylic acid moiety as donor part, in which the trend is reversed. The molar absorption coefficient of Dye-3 and Dye-4 are also higher than that of Dye-1 and Dye-2, but all of the values are still overwhelmingly higher than that of the reference dye N719 (1400 dm^3 mol^{-1} cm^{-1}). The performance of the dyes in DSSC is tabulated in Table 1 below as synthesised by Song et al. [79].

Table 1. Performance of DSSCs using dyes

Dye	V_{oc} (V)	J_{sc} (mA/cm^2)	ff	η (%)
N719	0.66	14.82	0.47	4.54
Dye-1	0.70	4.62	0.62	2.00
Dye-2	0.71	8.56	0.47	2.89
Dye-3	0.79	6.64	0.59	3.06
Dye-4	0.73	9.30	0.49	3.61

The V_{oc} of all the organic dyes are higher than N719 dye, which is theorised to occur due to inhibition of the charge recombination at the photoanode/dye/redox electrolyte interface and the semirigid phenylacetylene spacers. Dye-3 and Dye-4 with longer conjugation length achieved higher energy conversion efficiency than Dye-1 and Dye-2. The investigation on the effects of acetylene moiety as π-spacer on their properties and

DSSC performance also have been investigated prior [82]. They designed and synthesised four organic dyes containing acetylene moiety for comparison with five dyes without acetylene moiety (Figure 10). The dyes incorporating acetylene moiety exhibited red-shifting in their absorption spectrum due to the increased conjugation length, but the degree of re-shift in dyes with acetylene moiety is quite weaker compared to dyes with ethylene (double bond) moiety. Introduction of acetylene moiety only barely influenced the HOMO level of the dyes, but the dyes with ethylene moiety experienced negative shifting of its HOMO level.

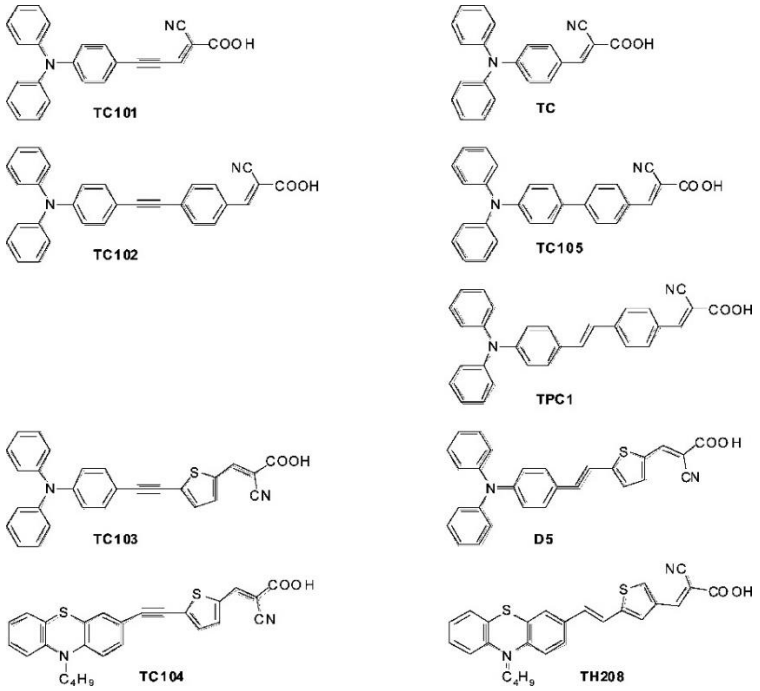

Figure 10. Dyes synthesised by Teng et al. [82] investigated the effects of acetylene moiety as π-spacer on their properties and DSSC performance.

Their designated DSSC performance of the dyes is tabulated in Table 2 below. Dyes with acetylene moiety only showed slight improvement in their energy conversion efficiency, compared to ethylene moiety which significantly improved the energy conversion efficiency, which is due to the lower J_{sc} of dyes containing acetylene moiety than dyes with ethylene moiety. But, DSSC using acetylene-based dyes showed improvement in their IPCE, due to the enhanced electron transfer yield of DSSC with introduction of triple bond.

Based on the selected studies, incorporation of acetylene moiety in dyes can induce red-shifting in their absorption spectrum via extension of conjugation length, which is important for the dye because more sunlight can be absorbed. Acetylene moiety also helped to improve the energy conversion efficiency of DSSC, but ethylene moiety showed much higher improvement in energy conversion efficiency. An advantage of acetylene moiety over ethylene moiety is their faster electron transfer yield, which enhance the IPCE of acetylene-based dye compared to ethylene-based dye. So, acetylene moiety can improve the properties of dyes and their DSSC performance, but more work needs to be done on the molecular design of dyes with acetylene moiety as linker in organic dyes, because ethylene moiety generally possesses better characteristics.

Table 2. Performance of synthesised dyes in DSSC

Dye	J_{sc} (mA·cm^{-2})	V_{oc} (V)	ff	η (%)
TC101	6.35	623	0.742	2.94
TC102	7.72	694	0.803	4.30
TC103	9.60	671	0.776	5.00
TC104	8.84	610	0.742	4.00
TC	5.26	636	0.776	2.60
TC105	7.58	693	0.773	4.06
TPC1	10.39	702	0.785	5.73
D5	12.41	663	0.760	6.25
TH208	11.99	643	0.743	5.73

Azomethine/Schiff base

Lokhande et al. [83] have come up with four new organic Schiff bases employing N-hexyl/N-phenyl carbazole moiety as a donor, 1-chlorobuta-1,3-diene as a π-bridge and 4-amino salicylic acid as acceptor for application as photosensitisers in DSSC (Figure 11). Incorporation of chlorine group along with additional π-bond worked effectively to improve the overall performance of dyes. Introduction of two acceptor units in 3b resulted in the decrement of HOMO-LUMO band gap with a bathochromic shift in absorption wavelength and broadening of the absorption spectrum. Introduction of hexyl unit in dyes exhibited better DSSC performance than the dyes with phenyl unit due to reduced aggregation of dye molecules on the TiO_2 surface [78].

Figure 11. Four those dyes designed and synthesised by Lokhande et al. in 2019 acting as photosensitisers in DSSC

In recent years, incorporation of theoretical studies on the physico-chemical and performance of these motifs are actively being performed. Particularly on the theoretical studies on the inclusion of azomethine moiety as linker in dye molecules. They investigated 10 dyes, of which three have already been reported experimentally and theoretically and of which seven are new structures inspired by the former. The effect of the pi-bridge was evaluated by combining azomethine, thiophene, and benzene derivatives using two and three units. In all cases, the inclusion of azomethine improved the electronic properties such as UV-Vis absorption, charge transfer from the donator part to acceptor part and the electron injection according to HOMO and LUMO levels, and chemical reactivity [84]. The incorporation of triphenylamine-thiopene based dyes with azomethine moieties as π-bridge, and their results showed that the dye with azomethine moieties were

capable of absorbing significant portion of light in the visible spectrum, suggesting its suitability for potential photovoltaic applications with further modification to its overall structure [85].

Heterocyclic

Heterocyclic is any cyclic organic compounds that contain at least one carbon atom with at least one other element such as nitrogen, oxygen and sulfur. In recent years, these compounds have been investigated greatly as spacer or linker in dyes for DSSCs applications. One of the derivatives of this heterocyclic moieties which has great potential to be utilized is known as isoindigo (Figure 12). It has been attracting great interest as an ideal building block for the electroactive materials for optoelectronics interest particularly in DSSCs. This is due to the fact that, it can afford high yields and turnovers [86]. Like other typical building block for organic electronics applications, it can be further developed into numerous molecular and polymeric materials with extended photophysical properties.

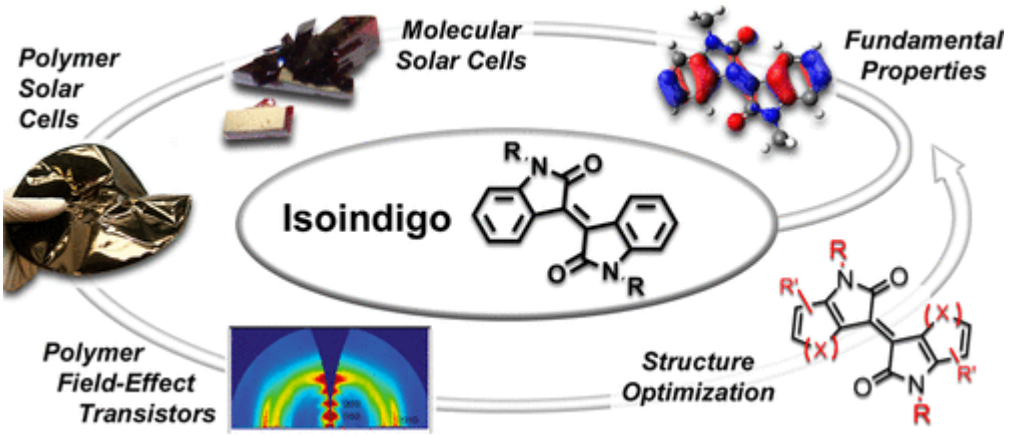

Figure 12. Numerous potential applications of isoindigo as building block in optoelectronics including in solar cells interests [86]

Isoindigo derivatives also have become a major focus recently in DSSCs acting as dyes. Synergistic studies involving computational approach of density functional theory (DFT) and the conventional experimental have become major interests among chemists and physicists in recent years. Hadsadee et al. [87] has utilized metal-free dyes based on isoindigo by performing DFT in order to improve efficiency in DSSCs. They have proposed triphenylamine as donor, thiophene as the π'-linker between the donor and auxiliary acceptor, and a phenyl or thiophene ring as the π-linker between the auxiliary acceptor and acceptor. The outcomes proven to exhibit good charge transfer properties and proven that the π-linker on photovoltaic would influence the performance in organic dyes.

By also incorporating DFT studies, a series of push−pull heterocyclic dyes of N, N diphenylhydrazones were prepared to study the effect of structural modifications with different π-spacers and electron withdrawing groups were studied further for their optical and non-linear properties. These derivatives were investigated for their potential as photosensitizers for nanocrystalline TiO_2-based DSSCs [88].

In designing and proposing well-performed DSSCs, the dyes should be highly efficient which the roles and influences of the donor (D) and acceptor (A) as well as ideal spacer or likers should be considered and chosen carefully. Due to its unique nature, heterocyclics containing sulfur and nitrogen like benzothiadiazole [89] were also explored and afforded great outcomes by altering the molecular backbones of the dyes. Similar computational method also can be utilised in other quite similar heterocyclic derivatives such as phenothiazine which in this study, the modification towards the bridging cores on their various properties such as structural, photovoltaic, electronic, and optical

properties were investigated further [90]. In 2020, a series of novel organic dyes containing bearing D-π-A system of phenothiazine were designed, synthesized and studied on their photophysical properties also pairing with DFT studies. It shows that, with the alteration on the substituents, the fundamental and thorough intramolecular charge transfers in these dyes can be understood further. [91]

Optical and redox properties of dyes are also essential features in photovoltaic studies. Incorporation of pyrrole and thiophenes in the molecular framework proven to that this sensitizer for DSSCs the best conversion efficiency up to 2.21%. This is mostly due to the contribution of the higher molar extinction coefficient, long π-conjugation of the heterocyclic system, higher oxidation potential and strong electron donating capacity of the ethoxyl group compared to the pirrolyl moiety [92].

With all the latest work and findings involving mixed moieties of D-πA system as dyes for DSSC and the greater impact these systems can contribute in solar cells studies, more exploration and in depth understanding on their fundamental features should be carried out. In recent years, typical experimental work paired with computational theoretical studies have shown that, a thorough details on the functionalities and performances of these developed DSSCs can be understood further. These two distinctive approaches are compatible to each other in supporting the development of an ideal usable DSSCs as an alternative green energy sources.

Conclusion and Future Outlook

There has been a thorough discussion on the fundamental aspects of DSSCs and other related elements featured in the build-up. The aim now is to explore various mixed moieties system that beneficial in term of extending the conjugation within the molecular framework of D-π-Acceptor system. The contribution of various substituents to the core of the molecules are also essential and may play a major role in giving the desired outcomes of the cells' efficiency and performances. In this contribution, a concise initial development of DSSC, its components and the overall working mechanism of the DSSC have been explored. Furthermore, the requirements for ideal organic dyes in DSSCs and the previous studies related to the application of acetylene and azomethine in dyes for DSSCs have been reviewed. Based on the reviewed works, dyes with acetylene, azomethine and heterocyclic mixed moieties have shown promising results for DSSC application and can be improved with further molecular tuning of the dyes. The ventures on the combination between these hybrid moieties as potential candidates as π-bridge in a dye molecule for DSSC should be taken into consideration Interestingly, focusing on the use of both acetylene and azomethine and taking highly elongated conjugation of these two can offer, there is no known research yet involving these moieties in individual molecular frameworks to date. Thus, the potentials are endless.

Acknowledgement

The authors would like to express gratitude to the Organisation for the Prohibition of Chemical Weapons (OPCW) (Grant numbers: 53309 (UMT's referral code), OPCW's Project Account No: L/ICA/ICB/217568/18) for research grant support, and Universiti Malaysia Terengganu for facilities and research aids.

References

1. Breeze, P. (2019). Power Generation Technologies (3rd ed.), Oxford: Elsevier: pp. 293-321.
2. World Energy Council (2013). World Energy Resources: Solar. https://www.worldenergy.org/assets/images/imported/2013/10/WER_2013_8_Solar_revised.pdf. [Access online 20 June 2023].
3. Ritchie, H. and Roser, M. (2020). Energy Production and Consumption. OurWorldInData. https://ourworldindata.org/energy-production-consumption. [Access online 20 June 2023].
4. Kumavat, P. P., Sonar, P. and Dalal, S. D. (2017). An overview on basics of organic and dye sensitized solar cells, their mechanism and recent improvements. *Renewable and Sustainable Energy Reviews*, 78: 1262- 1287.
5. Rhodes, C. J. (2010). Solar energy: Principles and possibilities. *Science Progress*, 93(1): 37-112.
6. American Physical Society (2009). This month in physics history - April 25, 1954: Bell Labs

demonstrates the first practical silicon solar cell. https://www.aps.org/publications/apsnews/200904/physicshistory.cfm. [Access online 4 May 2023].

7. Akinoglu, B. G., Tuncel, B. and Badescu, V. (2021). Beyond 3rd generation solar cells and the full spectrum project. Recent advances and new emerging solar cells. *Sustainable Energy Technologies and Assessments*. 46: 101287-101308.
8. Simke, W.C. (2019). Development of photovoltaic technologies for global impact. *Renewable Energy.* 138: 911-914.
9. Sharma, S., Jain, K. K. and Sharma, A. (2015). Solar cells: In research and applications—a review. *Materials Sciences and Applications,* 6(12): 1145-1155.
10. Badawy, W. A. (2015). A review on solar cells from Si-single crystals to porous materials and quantum dots. *Journal of Advanced Researchl,* 6(2): 123-132.
11. Tonui, P., Oseni, S. O., Sharma, G., Yan, Q. and Mola, G. T. (2018). Perovskites photovoltaic solar cells: An overview of current status. *Renewable and Sustainable Energy Reviews,* 91: 1025-1044.
12. Sharma, K., Sharma, V. and Sharma, S. S. (2018). Dye-sensitized solar cells: Fundamentals and current status. *Nanoscale Research Letters,* 13(381):1-46.
13. O'Regan, B. and Grätzel, M. (1991). A low cost, high-efficiency solar cell based on dye-sensitized colloidal TiO_2 films. *Nature.* 353: 737-740.
14. Lee, C.-P., Lin, C.-A., Wei, T.-C., Tsai, M.-L., Meng, Y., Li, C.-T., Ho, K.-C., Wu, C.-I, Lau, S.-P. and He, J.-H. (2015). Economical low-light photovoltaics by using the Pt-free dye-sensitized solar cell with graphene dot/PEDOT:PSS counter electrodes. *Nano Energy*, 18: 109-117.
15. Juang, S.S.-Y., Lin, P.-Y., Lin, Y.-C., Chen, Y.-S., Shen, P.-S., Guo, Y.-L., Wu, Y.-C. and Chen, P. (2019). Energy harvesting under dim-light condition with dye-sensitized and perovskite solar cells. *Frontiers in Chemistry*, 7(209):1-9.
16. Hagfeldt, A., Boschloo, G., Sun, L., Kloo, L. and Petterson, H. (2010). Dye-sensitized solar cells. *Chemical Reviews,* 110(11): 6595-6663.
17. Nazeeruddin, M. K. (2011). Dye-sensitized solar cells: A brief overview. *Solar Energy.* 85(6): 1172-1178.
18. Selvaraj, P., Baig, H., Mallick, T. K., Siviter, S., Montecucco, A., Li, W., Paul, M., Sweet, T., Gao, M., Knox, A. R. and Sundaram, S. (2018). Enhancing the efficiency of transparent dye-sensitized solar cells using concentrated light. *Solar Energy Materials and Solar Cells,* 175: 29-34.
19. Kakiage, K., Aoyama, Y., Yano, T., Oya, K., Fujisawa, J., and Hanaya, M. (2015). Highly-efficient dye-sensitized solar cells with collaborative sensitization by silyl-anchor and carboxy-anchor dyes. *Chemical Communications.* 51: 15894-15897.
20. Fraunhofer Institute for Solar Energy Systems ISE (2021). *Photovoltaics Report*. https://www.ise.fraunhofer.de/en/publications/studies/photovoltaics-report.html. [Access online 20 April 2023].
21. Grand View Research (2020). Dye sensitized solar cell market size, share & trends analysis report by application (portable charging, BIPV/BAPV, embedded electronics, outdoor advertising, automotive (AIPV)), and segment forecasts, 2020 – 2027. https://www.grandviewresearch.com/industry-analysis/dye-sensitized-solar-cell-market. [Access online 15 May 2023].
22. Belessiotis, G.V., Ibrahim, I., Karagianni, C. S. and Falaras, P. (2021). DSSCs for indoor environments: from lab scale experiments to real life applications. *SVOA Materials Science & Technology.* 3(1): 1-5.
23. Salton, J. (2009). World's first commercial application of DSSC solar technology is in the bag. New Atlas. https://newatlas.com/first-commercial-application-dssc-solar-technology/13100/. [Access online 20 June 2023].
24. Solaronix.com (2022). Solaronix - innovative solutions for solar professionals. https://solaronix.com. [Access online 20 June 2023].
25. Gong, J., Liang, J. and Sumathy, K. (2012). Review on dye sensitized solar cells (DSSCs): Fundamental concepts and novel materials. *Renewable and Sustainable Energy Reviews,* 16(8): 5848-5860.

26. Gorlov, M. and Kloo, L. (2008). Ionic liquid electrolytes for dye-sensitized solar cells. *Dalton Transactions.* 20: 2655-2666.
27. Yu, Z., Vlachopoulos, N., Gorlov, M. and Kloo, L. (2011). Liquid electrolytes for dye-sensitized solar cells. *Dalton Transactions.* 40: 10289-10303.
28. Bach, U., Lupo, D., Comte, P., Moser, J.E., Weissörtel, F., Salbeck, J., Spreitzer, H. and Grätzel, M. (1998). Solid-state dye-sensitized mesoporous TiO_2 solar cells with high photon-to-electron conversion efficiencies. *Nature.* 395: 583-585.
29. Boschloo, G. (2019). Improving the performance of dye-sensitized solar cells. *Frontiers in Chemistry*. 7(77):1-9.
30. Sun, K. C., Sahito, I. A., Noh, J. W., Yeo, S. Y., Im, J. N., Yi, S. C., Kim, Y. S. and Jeong, H. S. (2016). Highly efficient and durable dye-sensitized solar cells based on a wet-laid PET membrane electrolyte. *Journals of Materials Chemistry A*, 4(2): 458-465.
31. Karim, N. A., Mehmood, U., Zahid, H. F. and Asif, T. (2019). Nanostructured photoanode and counter electrode materials for efficient dye-sensitized solar cells (DSSCs). *Solar Energy*. 185: 165-188.
32. Papageorgiou, N. (2004). Counter-electrode function in nanocrystalline photoelectrochemical cell configurations. *Coordination Chemistry Reviews.* 248: 1421-1446.
33. Wu, J., Lan, Z., Lin, J., Huang, M., Huang, Y., Fan, L., Luo, G., Lin, Y., Xie, Y. and Wei, Y. (2017). Counter electrodes in dye-sensitized solar cells. *Chemical Society Reviews*. 46: 5975-6023.
34. Fang, X., Ma, T., Guan, G., Akiyama, M., Tetsuya, K. and Abe, E. (2004). Effect of the thickness of the Pt film coated on a counter electrode on the performance of a dye-sensitized solar cell. *Journal of Electroanalytical Chemistry*, 570(2): 257-263.
35. Thomas, S., Deepak, T. G., Anjusree, G. S., Arun, T. A., Nair, S. V. and Nair, A. S. (2014). A review on counter electrode materials in dye-sensitized solar cells. *Journal of Materials Chemistry A.* 2: 4474-4490.
36. Jeong, H., Pak, Y., Hwang, Y., Song, H., Lee, K. H., Ko, H.C. and Jung, G. Y. (2012). Enhancing the charge transfer of the counter electrode in dye-sensitized solar cells using periodically aligned platinum nanocups. *Small*, 8(24): 3757-3761.
37. Ahmad, M. S., Pandey, A. K. and Rahim, N. A. (2017). Advancements in the development of TiO_2 photoanodes and its fabrication methods for dye sensitized solar cell (DSSC) applications. A review. *Renewable and Sustainable Energy Reviews.* 77: 89-108.
38. Park, N.-G., van de Lagemaat, J. and Frank, A.J. (2000). Comparison of dye-sensitized rutile- and anatase-based TiO_2 solar cells. *The Journal of Physical Chemistry B*, 104(38): 8989-8994.
39. Kusumawati, Y., Hosni, M., Martoprawiro, M. A., Cassaignon, S. and Pauporté, T. (2014). Charge transport and recombination in TiO_2 brookite-based photoelectrodes. *The Journal of Physical Chemistry C*, 118(41): 23459-23467.
40. Mohammadian-Sarcheshmeh, H., Arazi, R. and Mazloum-Ardakani, M. (2020). Application of bifunctional photoanode materials in DSSCs: A review. *Renewable and Sustainable Energy Reviews.* 134: 110249-110250.
41. Raj, C.C. and Prasanth, R. (2016). A critical review of recent developments in nanomaterials for photoelectrodes in dye sensitized solar cells. *Journal of Power Sources.* 317: 120-132.
42. He, Y., Hu, J. and Xie, Y. (2015). High-efficiency dye-sensitized solar cells of up to 8.03% by air plasma treatment of ZnO nanostructures. *Chemical Communications*, 51(90): 16229-16232.
43. Chou, T.P., Zhang, Q., Russo, B., Fryxell, G.E. and Cao, G. (2007). Titania particle size effect on the overall performance of dye-sensitized solar cells. *The Journal of Physical Chemistry C*, 111(17): 6296-6302.
44. Dhungel, S. K. and Park, C. W. (2013). Impact of size distribution of nanoparticles in TiO_2 paste for its application in dye sensitized solar cells. *The Himalayan Physics*, 4(4): 27-31.
45. Wang, Z. S., Kawauchi, H., Kashima, T. and Arakawa, H. (2004). Significant influence of TiO_2 photoelectrode morphology on the energy conversion efficiency of N719 dye-sensitized solar cell. *Coordination Chemistry Reviews*, 248(13): 1381-1389.

46. Devadiga, D., Selvakumar, M., Shetty, P. and Santosh, M. S. (2021). Recent progress in dye sensitized solar cell materials and photo-supercapacitors: A review. *Journal of Power Sources,* 493: 229698-229755.
47. Dahlan, D., Saad, S. K. M., Berli, A. U., Bajili, A. and Umar, A. A. (2017). Synthesis of two-dimensional nanowall of Cu-doped TiO_2 and its application as photoanode in DSSCs. *Physica E,* 91: 185-189.
48. Mahmoud, M. S., Akhtar, M. S., Mohamed, I. M. A., Hamdan, R., Dakka, Y. A. and Barakat, N. A. M. (2018). Demonstrated photons to electron activity of S-doped TiO_2 nanofibers as photoanode in the DSSC. *Materials Letters,* 225: 77-81.
49. Prabavathy, N., Balasundaraprabhu, R., Balaji, G., Malikaramage, A. U., Prasanna, S., Sivakumaran, K., Kumara, G. R. A., Rajapakse, R. M. G. and Velauthapillai, D. (2019). Investigations on the photo catalytic activity of calcium doped TiO_2 photo electrode for enhanced efficiency of anthocyanins-based dye sensitized solar cells. *Journal of Photochemistry & Photobiology A: Chemistry*, 377: 43-57.
50. Chen, X., Du, Q., Yang, W., Liu, W., Miao. Z. and Yang, P. (2017). A double-layered photoanode made of ZnO/TiO_2 composite nanoflowers and TiO_2 nanorods for high efficiency dye-sensitized solar cells. *Journal of Solid State Electrochemistry*, 22: 685-691.
51. Bakr, Z. H., Wali, Q., Ismail, J., Elumalai, N. K., Uddin, A. and Jose, R. (2018). Synergistic combination of electronic and electrical properties of SnO_2 and TiO_2 in a single SnO_2-TiO_2 composite nanofiber for dye-sensitized solar cells. *Electrochimica Acta,* 263: 524-532.
52. Chatterjee, S., Webre, W. A., Patra, S., Rout, B., Glass, G. A., D'Souza, F. and Chatterjee, S. (2020). Achievement of superior efficiency of TiO_2 nanorod-nanoparticle composite photoanode in dye sensitized solar cell. *Journal of Alloys and Compounds.* 826: 154188-154196.
53. Zhang, S., Yang, X., Numata, Y. and Han, L. (2013). Highly efficient dye-sensitized solar cells: Progress and future challenges. *Energy & Environmental Science,* 6: 1443-1464.
54. Bhattacharya, S. and John, S. (2019). Beyond 30% conversion efficiency in silicon solar cells: A numerical demonstration. *Scientific Reports.* 9: 12482-12497.
55. Shalini, S., Balasundaraprabhu, R., Kumar, T. S., Prabavathy, N., Senthilarasu, S. and Prasanna, S. (2016). Status and outlook of sensitizers/dyes used in dye sensitized solar cells (DSSC): A review. *International Journal of Energy Research,* 40(10): 1303-1320.
56. Galoppini, E. (2004). Linkers for anchoring sensitizers to semiconductor nanoparticles. *Coordination Chemistry Reviews,* 248: 1283-1297.
57. Zhang, L. and Cole, J. M. (2015). Anchoring groups for dye-sensitized solar cells. *ACS Applied Materials & Interfaces*, 7(6): 3427-3455.
58. Cahen, D., Hodes, G., Grätzel, M., Guillemoles, J. F. and Riess, I. (2000). Nature of photovoltaic action in dye-sensitized solar cells. *The Journal of Physical Chemistry B,* 104(9): 2053-2059.
59. Ooyama, Y. and Harima, Y. (2012). Photophysical and electrochemical properties, and molecular structures of organic dyes for dye-sensitized solar cells. *ChemPhysChem,* 13(18): 4032-4080.
60. Asghar, M. I., Miettunen, K., Halme, J., Vahermaa, P., Toivola, M., Aitola, K. and Lund, P. (2010) Review of stability for advanced dye solar cells. *Energy & Environmental Science,* 3(4): 418-426.
61. Nazeeruddin, M. K., Kay, A., Rodicio, I., Humphry-Baker, R., Müller, E., Liska, P., Vlachopoulos, N. and Grätzel, M. (1993). Conversion of light to electricity by *cis*-X_2Bis(2,2'-bipyridyl-4,4'-dicarboxylate)ruthenium(II) charge-transfer sensitizers (X = Cl^-, Br^-, I^-, CN^-, and SCN^-) on nanocrystalline TiO_2 electrodes. *Journal of the American Chemical Society,* 115(14): 6382-6390.
62. Nazeeruddin, M. K., Zakeeruddin, S. M., Humphry-Baker, R., Jirousek, M., Liska, P., Vlachopoulos, N., Shklover, V., Fischer, C.-H. and Grätzel, M. (1999). Acid-base equilibria of (2,2-bipyridyl-4,4-dicarboxylic acid)ruthenium(II) complexes and the effect of protonation on charge-transfer sensitization of nanocrystalline titania. *Inorganic Chemistry,* 38(26): 6298-6305.
63. Swetha, T., Reddy, K. R. and Singh, S. P. (2015). Osmium polypyridyl complexes and their

applications to dye-sensitized solar cells. *The Chemical Records*, 15(2): 457-474.

64. Sauvé, G., Cass, M. E., Coia, G., Doig, S. J., Lauermann, I., Pomykal, K. E. and Lewis, N. S. (2000). Dye sensitization of nanocrystalline titanium dioxide with osmium and ruthenium polypyridyl complexes. *The Journal of Physical Chemistry B*, 104(29): 6821-6836.
65. Alebbi, M., Bignozzi, C. A., Heimer, T. A., Hasselmann, G. M. and Meyer, G. J. (1998). The limiting role of iodide oxidation in cis-$Os(dcb)_2(CN)_2/TiO_2$ photoelectrochemical cells. *The Journal of Physical Chemistry B*, 102(39): 7577-7581.
66. Kuciauskas, D., Freund, M. S., Gray, H. B., Winkler, J. R. and Lewis, N. S. (2001). Electron transfer dynamics in nanocrystalline titanium dioxide solar cells sensitized with ruthenium or osmium polypyridyl complexes. *The Journal of Physical Chemistry B*, 105(2): 392-403.
67. Islam, A., Sugihara, H., Hara, K., Singh, L. P., Katoh, R., Yanagida, M., Takahashi, Y., Murata, S. and Arakawa, H. (2000). New platinum(II) polypyridyl photosensitizers for TiO_2 solar cells. *New Journal of Chemistry*. 24(6): 343-345.
68. Siu, C.-H., Lee, L.T.L., Yiu, S.-C., Ho, P.-Y., Zhou, P., Ho, C.-L., Chen, T., Liu, J., Han, K. and Wong, W.-Y. (2015). Synthesis and characterization of phenothiazine-based platinum(II)–acetylide photosensitizers for efficient dye-sensitized solar cells. *Chemistry: A European Journal*. 22: 3750-3757.
69. Dai, F.-R., Chen, Y.-C., Lai, L.-F., Wu, W.-J., Cui, C.-H., Tan, G.-P., Wang, X.-Z., Lin, J.-T., Tian, H. and Wong, W.-Y. (2012). Unsymmetric platinum(II) bis(aryleneethynylene) complexes as photosensitizers for dye-sensitized solar cells. *Chemistry: An Asian Journal*, 7(6): 1426-1434.
70. Lee, C.-P., Li, C.-T. and Ho, K.-C. (2017). Use of organic materials in dye-sensitized solar cells. *Materials Today*, 20(5): 267-283.
71. Yahya, M., Bouziani, A., Ocak, C., Seferoğlu, Z. and Sillanpää, M. (2021). Organic/metal-organic photosensitizers for dye-sensitized solar cells (DSSC): Recent developments, new trends, and future perceptions. *Dyes and Pigments*, 192: 109227-109265.
72. Ning, Z., Fu, Y. and Tian, H. (2010). Improvement of dye-sensitized solar cells: what we know and what we need to know. *Energy & Environmental Science*, 3(9): 1170-1181.
73. Kim, B.-G., Chung, K. and Kim, J. (2013). Molecular design principle of all-organic dyes for dye-sensitized solar cells. *Chemistry - A European Journal*, 19(17): 5220-523.
74. Ndaleh, D. N. D., Nugegoda, D., Watson, J., Cheema, H. and Delcamp, J. H. (2021). Donor group influence on dye-sensitized solar cell device performances: balancing dye loading and donor size. *Dyes and Pigments*, 187: 109074-109082.\
75. Mahmood, A., Khan, S.U.-D., Rana, U.A. and Tahir, M.H. (2019). Red shifting of absorption maxima of phenothiazine based dyes by incorporating electron-deficient thiadiazole derivatives as p-spacer. *Arabian Journal of Chemistry*, 12(7): 1447-1453.
76. Yu, Q.-Y., Liao, J.-Y., Zhou, S.-M., Shen, Y., Liu, J.-M., Kuang, D.-B. and Su, C.-Y. (2011). Effect of hydrocarbon chain length of disubstituted triphenyl-amine-based organic dyes on dye-sensitized solar cells. *The Journal of Physical Chemistry C*, 115(44): 22002-22008.
77. Khairul, W. M., Wahab, F. F. A., Che Soh, S. K., Shamsuddin, M. and Daud, A. I., (2020). Palladium(II)-pivaloyl thiourea complexes: synthesis, characterisation and their catalytic activity in mild Sonogashira cross-coupling reaction. *Chemical Physics Letters*, 756: 137842-137850.
78. Zaini, M. F., Khairul, W. M., Arshad, S., Abdullah, M., Zainuri, D. A., Rahamathullah, R., Rosli, M. I., Aziz, M. S. A. and Razak, I. A. (2020). The structure-property studies and mechanism of optical limiting action of methyl 4-((4-aminophenyl)ethynyl)benzoate crystal under continuous wave laser excitation. *Optical Materials*, 107: 110087-110105.
79. Song, J., Zhang, F., Li, C., Liu, W., Li, B., Huang, Y. and Bo, Z. (2009). Phenylethyne-bridged dyes for dye-sensitized solar cells. *The Journal of Physical Chemistry C*, 113(30): 13391-13397.

80. Jasman, S. M., Khairul, W.M., Tagg, T., Kubulat, K., Rahamathullah R., Arshad, S., Razak, I. A. and Tahir, M. I. M. (2015). Synthesis, crystal structure, and electrical studies of naphthoyl-thiourea as potential organic light emitting diode, *Journal of Chemical Crystallography*, 45: 338-349.
81. Lee, S. T., Khairul, W. M., Lee, O. J., Rahamathullah, R., Daud, A. I., Ku Bulat, K. H., Sapari, S., Razak, F. A. I and Krishnan, G. (2021). Electronic, reactivity and third order nonlinear optical properties of thermally-stable push-pull chalcones for optoelectronic interest: experimental and DFT assessments. *Journal of Physics and Chemistry of Solids*, 159: 110276-110290.
82. Teng, C., Yang, X., Yang, C., Tian, H., Li, S., Wang, X., Hagfeldt, A. and Sun, L. (2010). Influence of triple bonds as π-spacer units in metal-free organic dyes for dye-sensitized solar cells. *The Journal of Physical Chemistry C*, 114(25): 11305-11313.
83. Lokhande, P.K.M., Sonigara, K.K., Jadhav, M.M., Patil, D.S., Soni, S.S. and Sekar, N. (2019). Multi-dentate carbazole based schiff base dyes with chlorovinylene group in spacer for dye-sensitized solar cells: A combined theoretical and experimental study. *Chemistry Select*, 4(14): 4044-4056.
84. Delgado-Montiel, T., Soto-Rojo, R., Baldenebro-López, J. and Glossman-Mitnik, D. (2019). Theoretical study of the effect of different π bridges including an azomethine group in triphenylamine-based dye for dye-sensitized solar cells. *Molecules*, 24(21): 3897-3913.
85. Sarswat, P. K., Sathyapalan, A., Zhu, Y. and Free, M. L. (2013). Design, synthesis, and characterization of TPA-thiophene-based amide or imine functionalized molecule for potential optoelectronic devices. *Journal of Theoretical and Applied Physics*, 7(4):1-9.
86. Stalder, R., Mei, J., Graham, K. R., Estrada, L. A. and Reynolds, J. R. (2014). Isoindigo, a versatile electron-deficient unit for high-performance organic electronics. *Chemistry of Materials*, 26(1): 664-678.
87. Hadsadee, S., Promarak, V., Sudyoadsuk, T., Keawin, T., Kungwan, N. and Jungsuttiwong, S. (2020). Theoretical study on factors influencing the efficiency of *d–π′–a′–π–a* isoindigo-based sensitizer for dye-sensitized solar cells. *Journal of Electronic Materials*, 49: 318-332.
88. Fernandes, S. S. M., Belsley, M., Pereira, A. I., Ivanou, D., Mendes, A., Justino, L. L. G., Burrows, H. D. and Raposo, M. M. M. (2018). Push−pull n,n-diphenylhydrazones bearing bithiophene or thienothiophene spacers as nonlinear optical second harmonic generators and as photosensitizers for nanocrystalline TiO_2 dye sensitized solar cells. *ACS Omega*, 3: 12893-12904.
89. Mustafa, F. M., Abdel-Latif, M. K., Abdel-Khalek, A. A. and Kühn, O. (2023). Efficient D-π-π-A-type dye sensitizer based on a benzothiadiazole moiety: A computational study. *Molecules*, 28(13): 5185-5197.
90. Kacimi, R., Raftani, M., Abram, T., Azaid, A., Ziyat, H., Bejjit, L., Bennani, M. N., and Bouachrine, M. (2021). Theoretical design of D-π-A system new dyes candidate for DSSC application. *Heliyon*, 7: e07171-e707181.
91. Mantur, S., Patil, M. K., Nadaf, A. A., Najare, M. S., Yaseen, M., Inamdar, S. R. and Khazi, I. A. (2020). Synthesis, characterization and photophysical properties of π-conjugated novel phenothiazine substituted acrylonitrile D–A derivatives: Orange to red emission. *Chemical Data Collections*, 30: 100543-100556.
92. Fernandes, S. S. M., Castro, M. C. R., Ivanou, D., Mendes, A. and Raposo, M. M. M. (2022). Push-pull heterocyclic dyes based on pyrrole and thiophene: Synthesis and evaluation of their optical, redox and photovoltaic properties. *Coatings*, 12: 34-46.